How the Pauli exclusion principle affects fusion of atomic nuclei

C. Simenel,[1,*] A.S. Umar,[2,†] and K. Godbey[2,‡]

[1]*Department of Nuclear Physics, Research School of Physics and Engineering, The Australian National University, Canberra ACT 2601, Australia*

[2]*Department of Physics and Astronomy, Vanderbilt University, Nashville, TN 37235, USA*

(Dated: August 24, 2016)

The Pauli exclusion principle induces a repulsion between composite systems of identical fermions such as colliding atomic nuclei. Our goal is to study how heavy-ion fusion is impacted by Pauli repulsion. We propose a new microscopic approach, the density-constrained frozen Hartree-Fock method, to compute the bare potential including the Pauli exclusion principle exactly. Coupled-channel calculations show a reduction of fusion cross-section around the barrier due to Pauli repulsion, leading to a good agreement with experimental fusion cross-sections for up to eight orders of magnitude. Pauli repulsion provides a plausible explanation for the long-standing deep sub-barrier fusion hindrance problem.

The idea that identical fermions cannot occupy the same quantum state was proposed by Stoner [1] and generalized by Pauli [2]. Known as the Pauli exclusion principle, it was at first empirical, but is now explained by the spin-statistic theorem in quantum field theory [3, 4]. The importance of the Pauli exclusion principle cannot be overstated. For instance, it is largely responsible for the stability of matter against collapse, as demonstrated by the existence of white dwarves. It also generates a repulsion between composite systems of identical fermions at short distance. For instance, it repels atomic electron clouds in ionic molecules due to the fermionic nature of the electron. Another example is the hard-core repulsion between two nucleons induced by identical quarks of same color present in both nucleons. Naturally, a similar effect is expected to occur between atomic nuclei which are composite systems of nucleons. Indeed, it has been predicted that the Pauli exclusion principle should induce a repulsion (called "Pauli repulsion" hereafter) between strongly overlapping nuclei [5].

The Pauli repulsion should then be included in the nucleus-nucleus potential used to model reactions such as (in)elastic scattering, (multi)nucleon transfer, and fusion. However, Pauli repulsion is usually neglected in these models: It has been argued that the outcome of a collision between nuclei is mostly determined at a distance where the nuclei do not overlap much and thus the effects of the Pauli exclusion principle are minimum. This argument is based on the assumption that nuclei do not necessarily probe the inner part of the fusion barrier induced by the competition between Coulomb repulsion and strong nuclear attraction. However, at energies well above the barrier, the system could reach more compact shapes where one cannot neglect the effect of the Pauli principle anymore, as was shown by several authors in the 1970's [5–8]. Similarly, deep sub-barrier fusion should depend on the potential inside the barrier [9].

Using a realistic approach to fusion based on microscopic and coupled-channel (CC) calculations, we show that, in fact, the Pauli repulsion is playing an important role on fusion from deep sub-barrier to above barrier energies. In particular, it provides a natural explanation for the experimentally observed deep sub-barrier fusion hindrance [10–12] (see Ref. [13] for a review) which has led to various theoretical interpretations [11, 14–19], although none of them directly consider Pauli repulsion as a possible mechanism.

In order to investigate the effect of Pauli repulsion on heavy-ion fusion, we introduce a novel microscopic method called density-constrained frozen Hartree-Fock (DCFHF) to compute the interaction between nuclei while accounting exactly for the Pauli exclusion principle between nucleons. The microscopically derived bare nucleus-nucleus potential including Pauli repulsion is then used in CC calculations. As an example, ^{40}Ca+^{40}Ca, ^{48}Ca+^{48}Ca and ^{16}O+^{208}Pb fusion cross-sections are computed without any parameter adjustment, and compared with experimental data.

To avoid the introduction of new parameters, we adopt the idea of Brueckner et al [20] to derive the bare potential from an energy density functional (EDF) $E[\rho]$ written as an integral of an energy density $\mathscr{H}[\rho(\mathbf{r})]$, i.e.,

$$E[\rho] = \int \mathrm{d}\mathbf{r}\, \mathscr{H}[\rho(\mathbf{r})]. \tag{1}$$

The bare potential is obtained by requiring frozen ground-state densities ρ_i of each nucleus ($i = 1,2$) which we compute using the Hartree-Fock (HF) mean-field approximation [21, 22]. The Skyrme EDF [23] is used both in HF calculations and to compute the bare potential. It accounts for the bulk properties of nuclear matter such as its incompressibility which is crucial at short distances [14, 20, 24]. Neglecting the Pauli exclusion principle between nucleons in different nuclei leads to the usual frozen Hartree-Fock (FHF) potential [25–28]

$$V_{FHF}(\mathbf{R}) = \int \mathrm{d}\mathbf{r}\, \mathscr{H}[\rho_1(\mathbf{r}) + \rho_2(\mathbf{r}-\mathbf{R})] - E[\rho_1] - E[\rho_2], \tag{2}$$

where $\mathbf{R}$ is the distance vector between the centers of mass of the nuclei. The FHF potential, assumed to be central, can then directly be used to compute fusion cross-sections in CC calculations accounting for dynamical reorganisation of the nuclei due to collective excitations [29–31] (see [32] for a review of the CC method).

Our new DCFHF method is the static counter-part of the density-constrained time-dependent Hartree-Fock approach

developed to extract the nucleus-nucleus potential of dynamically evolving systems [33]. In particular, this approach shows that the Pauli exclusion principle splits orbitals such that some states contribute attractively (bounding) and some repulsively (antibounding) to the potential [34]. In the present method, it is important that the nuclear densities remain frozen in the densities of the HF ground-states of the collision partners in order to extract the bare potential, i.e., without polarization effects which are included in a second step in the CC calculations. Thus, the DCFHF approach allows to compute the bare potential by using the self-consistent HF mean-field with exact frozen densities. The Pauli exclusion principle is included exactly by allowing the single-particle states, comprising the combined nuclear density, to reorganize to attain their minimum energy configuration and be properly antisymmetrized as the many-body state is a Slater determinant of all the occupied single-particle wave-functions. The HF minimization of the combined system is thus performed subject to the constraint that the local proton (p) and neutron (n) densities do not change:

$$\delta\langle H - \sum_{q=p,n}\int d\mathbf{r}\,\lambda_q(\mathbf{r})\,[\rho_{1_q}(\mathbf{r})+\rho_{2_q}(\mathbf{r}-\mathbf{R})]\,\rangle = 0\,, \quad (3)$$

where the $\lambda_{n,p}(\mathbf{r})$ are Lagrange parameters at each point of space constraining the neutron and proton densities. This equation determines the state vector (Slater determinant) $|\Phi(\mathbf{R})\rangle$. The DCFHF potential, assumed to be central, is then defined as

$$V_{\rm DCFHF}(R) = \langle\Phi(\mathbf{R})|H|\Phi(\mathbf{R})\rangle - E[\rho_1] - E[\rho_2]\,. \quad (4)$$

Calculations were done in a three-dimensional Cartesian geometry with no symmetry assumptions using a static version of the code of Ref. [40] and using the Skyrme SLy4d interaction [41] which has been successful in describing various types of nuclear reactions [28]. The three-dimensional Poisson equation for the Coulomb potential is solved by using Fast-Fourier Transform techniques and the Slater approximation is used for the Coulomb exchange term. The static HF equations and the DCFHF minimizations are implemented using the damped gradient iteration method. The box size used for all the calculations was chosen to be $60\times30\times30$ fm^3, with a mesh spacing of 1.0 fm in all directions. These values provide very accurate results due to the employment of sophisticated discretization techniques [42, 43].

The FHF (solid line) and DCFHF (dashed line) potentials are shown in Figs. 1(a-c) for ^{16}O+^{208}Pb, ^{40}Ca+^{40}Ca, and ^{48}Ca+^{48}Ca systems, respectively. It is observed that the Pauli exclusion principle (present only in DCFHF) induces a repulsion at short distance in the three systems. The resulting effects are negligible outside the barrier and relatively modest near the barrier, with an increase of the barrier height by $\sim 1-2\%$ and a reduction of its radius by $\sim 2-4\%$ due to Pauli repulsion. However, the impact is more important in the inner barrier region, with the production of a potential pocket at short distance. As a result, the barrier width is increased. Pauli repulsion is then expected to reduce the sub-barrier tunnelling probability as the latter decreases exponentially with the barrier width.

The Pauli repulsion potential can be extracted from $V_{Pauli}(R) = V_{DCFHF}(R) - V_{FHF}(R)$. It is plotted in Fig. 2 as a function of $R - R_B^{FHF}$ where the FHF barrier radius R_B^{FHF} is used as a reference. An exponential decrease is observed in all systems. A shift is also observed between the calcium systems which is essentially due to the neutron skin in ^{48}Ca increasing R_B. The exponential decrease can be explained with a simple model for the ^{48}Ca+^{48}Ca system as it is symmetric and the density at the surface of ^{48}Ca is essentially determined by the $1f_{7/2}$ neutrons which are not affected by long-range Coulomb interaction. In this case, the behaviour of the density at large distance r can be approximated by $\rho(r) \sim \frac{e^{-2\kappa_0 r}}{(\kappa_0 r)^2}$ (see, e.g., [44]), where $\kappa_0 = \sqrt{-2m\varepsilon_0}/\hbar$, m is the nucleon mass, and $\varepsilon_0 \simeq -9.55$ MeV is the energy of the $1f_{7/2}$ neutron orbital in our HF calculations. The Pauli repulsion is expected to go as the square of the overlap of the wave-functions [5], leading to

$$V_{Pauli}(R) \sim \left|\int d\mathbf{r}\,\frac{e^{-\kappa_0 r}}{r}\,\frac{e^{-\kappa_0|\mathbf{R}-\mathbf{r}|}}{|\mathbf{R}-\mathbf{r}|}\right|^2 \sim \frac{e^{-2\kappa_0 R}}{R^4} \quad (5)$$

for large R. This expression is used to fit V_{Pauli} for $R > R_B^{FHF}$ (with only the magnitude of the potential as a free parameter). The result, shown with a dotted-dashed line in Fig. 2, gives an excellent reproduction of the form of the potential down to ~ 2 fm inside the barrier.

In principle, the Pauli repulsion is expected to be energy dependent. One source of energy dependence is the reduction of the overlap between wave functions with relative kinetic momentum, reducing the Pauli repulsion at high energy [5, 6, 8, 45]. Other sources are the current density dependence of the EDF (needed for Galilean invariance) [6] and non-local effects of the Pauli exclusion principle leading to an energy dependence of the local equivalent potential [46]. These effects, however, are expected to affect the Pauli repulsion at energies much higher than the barrier, and can then be neglected in near barrier fusion studies.

We have also tested other methods to account for Pauli repulsion in the bare potential. For instance, antisymmetrizing overlapping ground-state wave-functions [5–7] can be done with a Gram-Schmidt procedure. Although the resulting potential properly accounts for the Pauli exclusion principle, it leads to much higher repulsion as illustrated in Fig. 1(b) (dotted-dashed line) for the ^{40}Ca+^{40}Ca system in which the potential pocket, and therefore the fusion barrier, simply disappear. Let us use a simple model to explain the origin of this large repulsion. Consider two single-particle wave functions $\varphi_{1,2}$ belonging to the HF ground-states of the two different nuclei and which have a small overlap in the neck region at $\mathbf{r}_0$ only: $\varphi_1^*(\mathbf{r})\varphi_2(\mathbf{r}) \simeq \alpha\delta(\mathbf{r}-\mathbf{r}_0)$. By definition, the total frozen density of these two nucleons is $\rho_F = |\varphi_1|^2 + |\varphi_2|^2$. The evaluation of observables, however, requires antisymmetrized wave-functions such as $\tilde{\varphi}_\pm = \mathcal{N}_\pm(\varphi_1 \pm \varphi_2)$ with

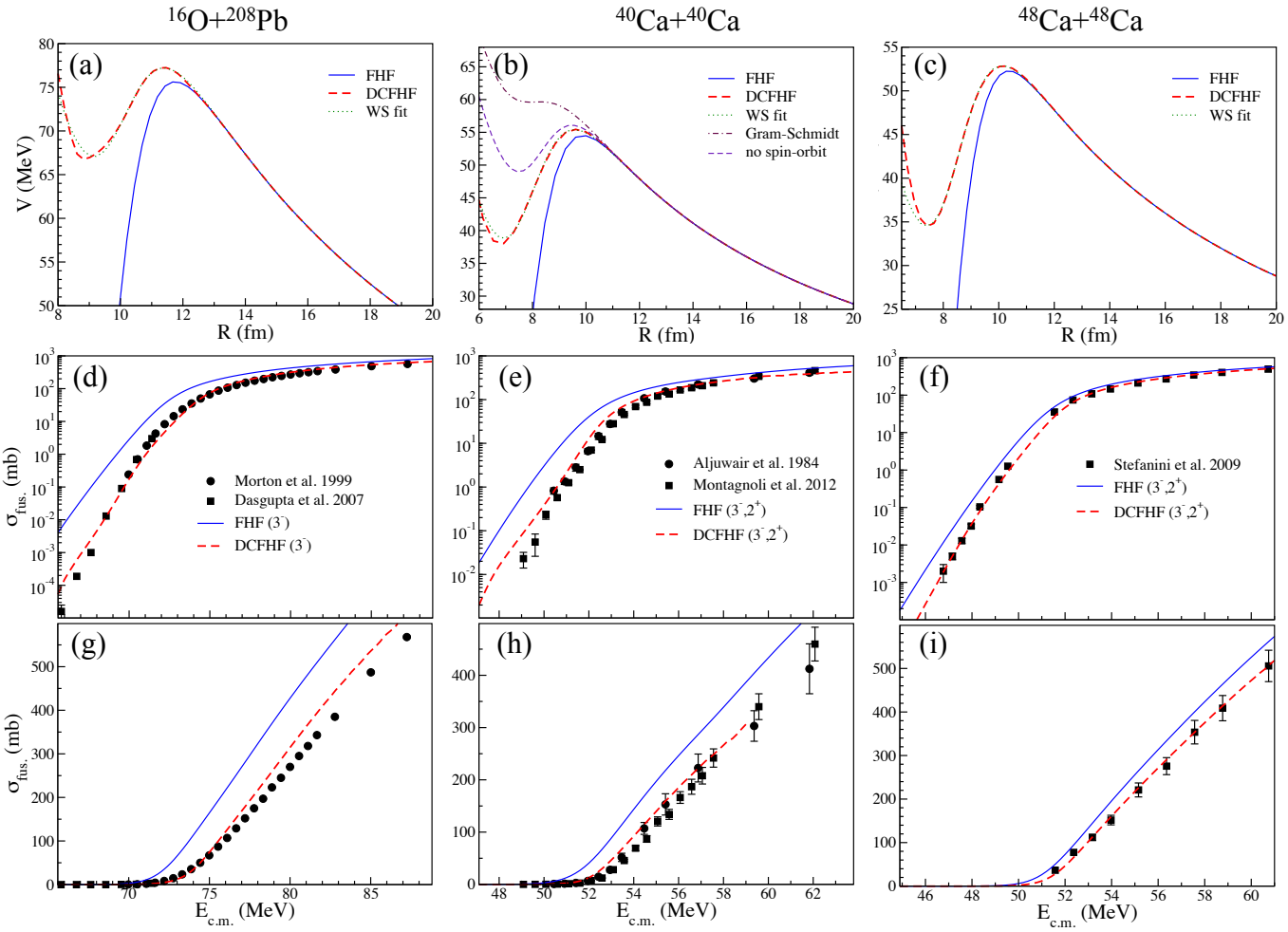

FIG. 1. (Color online) (a-c) Nucleus-nucleus potential from FHF (solid line) and DCFHF (dashed line) together with its Woods-Saxon fit (dotted line). Fusion cross-sections from the CCFULL code [35] are plotted in logarithmic (d-f) and linear scales (g-i) using the FHF (solid line) and DCFHF (dashed line) potentials. Cross-sections with the DCFHF potential are not shown above 59 MeV in panel (h) due to numerical instabilities visible in linear scale. Experimental data are from Refs. [11, 36–39].

normalization coefficients $\mathcal{N}_\pm = (2 \pm \alpha \pm \alpha^*)^{-1/2}$ and overlaps $\langle \tilde{\varphi}_- | \tilde{\varphi}_+ \rangle = 0$. The corresponding density reads $\tilde{\rho} = |\tilde{\varphi}_+|^2 + |\tilde{\varphi}_-|^2 \simeq \rho_F - \frac{1}{2}(\alpha + \alpha^*)^2 \delta(\mathbf{r} - \mathbf{r}_0)$. It is reduced in the neck compared to the frozen density and thus leads to a smaller nuclear attraction between the nuclei or, equivalently, to a spurious repulsion between the fragments as seen in Fig. 1(b). Naive antisymmetrization procedures are then not compatible with the frozen density picture.

Let us now discuss another traditional method which is to account for Pauli repulsion simply by increasing the kinetic energy density $\tau(\mathbf{r})$ (e.g., via the Thomas-Fermi model) [6–8, 47, 48]. This method would be valid if the effect of the Pauli exclusion principle was only to rearrange the kinetic energy term $\frac{\hbar^2}{2m}\tau$ without impacting other terms of the functional. In fact, the EDF also depends on τ via the "$t_{1,2}$" momentum dependent terms of the Skyrme effective interaction and, then, a variation of $\tau(\mathbf{r})$ also affects the nuclear part of the potential [6, 47]. Interestingly, we have also observed that including the Pauli exclusion principle has a strong impact on the spin-orbit energy. This is illustrated in Fig. 1(b) for the ^{40}Ca+^{40}Ca system. For this system, removing the spin-orbit interaction has little impact on the FHF potential (not shown in the figure), but strongly increases the repulsion between the fragments in the DCFHF potential (thin dashed line). This shows that the spin-orbit energy absorbs a large part of the Pauli repulsion. Thus, the Pauli exclusion principle has a more complicated effect than just increasing the kinetic energy density.

Coupled-channels calculations were performed with the CCFULL code [35] using Woods-Saxon fits of the FHF and DCFHF potentials (shown by dotted lines in Figs. 1(a-c) for the DCFHF potentials). By default, the incoming wave boundary condition (IWBC) is used. For shallow pocket potentials, however, the IWBC should be replaced by an imaginary potential inside the barrier to avoid numerical instabilities. This is done for calculations with the ^{16}O+^{208}Pb DCFHF potential using a modified version of CCFULL. Couplings to the low-lying collective 2^+ (in calcium isotopes) and 3^- states

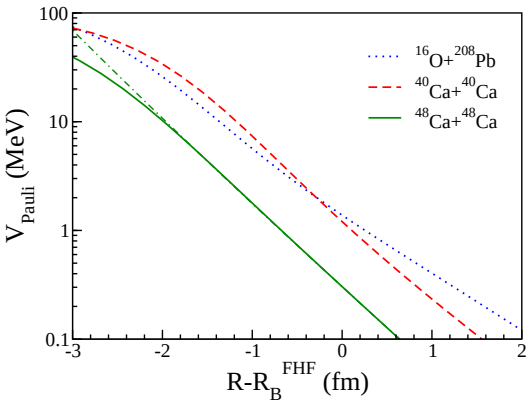

FIG. 2. (Color online) Pauli repulsion potential extracted from the difference between the DCFHF and FHF potentials. The dotted-dashed line is obtained from Eq. (5) (see text).

are included with standard values of the coupling constants [36, 49]. One (two) vibrational mode(s) can be included in the projectile (target). For the 2^+ states, we then use the fact that, for symmetric systems, the mutual excitation of one-phonon states in both nuclei can be approximated by one phonon with a coupling constant scaled by $\sqrt{2}$ [50].

Fusion cross sections are plotted in Figs. 1(d-f) and (g-i) in logarithmic and linear scales, respectively, for an energy range of $\pm 15\%$ around V_B^{DCFHF}. Calculations with the FHF potential systematically overestimate the data while the DCFHF potential leads to a much better agreement with experiment at all energies, and over up to 8 orders of magnitude in cross-sections. This shows the importance of taking into account Pauli repulsion in the bare potential for fusion calculations. We emphasise that these calculations are performed without adjustable parameters. However, the CC calculations are kept simple and include only the most relevant couplings. Improvements could be obtained, e.g., by including anharmonicity of the multi-phonon states [51]. Interestingly, the agreement between theory and data remains good at deep sub-barrier energies once Pauli repulsion is included. Thus, the Pauli exclusion principle provides a plausible explanation for the long-standing deep sub-barrier fusion hindrance problem [10–13].

Discussions with D. J. Hinde and M. Dasgupta are acknowledged. This work has been supported by the Australian Research Council Grant No. FT120100760, and by the U.S. Department of Energy under grant No. DE-SC0013847 with Vanderbilt University.

* cedric.simenel@anu.edu.au
† umar@compsci.cas.vanderbilt.edu
‡ kyle.s.godbey@vanderbilt.edu

[1] E. C. Stoner, Phil. Mag. **48**, 719 (1924).
[2] W. Pauli, Z. Phys. **31**, 765 (1925).
[3] M. Fierz, Helv. Phys. Acta **12**, 3 (1939).
[4] W. Pauli, Phys. Rev. **58**, 716 (1940).
[5] T. Fliessbach, Z. Phys. **247**, 117 (1971).
[6] D. M. Brink and F. Stancu, Nucl. Phys. A **243**, 175 (1975).
[7] P. Zint and U. Mosel, Phys. Lett. B **56**, 424 (1975).
[8] F. Beck, K.-H. Müller, and H. S. Köhler, Phys. Rev. Lett. **40**, 837 (1978).
[9] C. H. Dasso and G. Pollarolo, Phys. Rev. C **68**, 054604 (2003).
[10] C. L. Jiang, H. Esbensen, K. E. Rehm, B. B. Back, R. V. F. Janssens, J. A. Caggiano, P. Collon, J. Greene, A. M. Heinz, D. J. Henderson, I. Nishinaka, T. O. Pennington, and D. Seweryniak, Phys. Rev. Lett. **89**, 052701 (2002).
[11] M. Dasgupta, D. J. Hinde, A. Diaz-Torres, B. Bouriquet, C. I. Low, G. J. Milburn, and J. O. Newton, Phys. Rev. Lett. **99**, 192701 (2007).
[12] A. M. Stefanini, G. Montagnoli, L. Corradi, S. Courtin, E. Fioretto, A. Goasduff, F. Haas, P. Mason, R. Silvestri, P. P. Singh, F. Scarlassara, and S. Szilner, Phys. Rev. C **82**, 014614 (2010).
[13] B. B. Back, H. Esbensen, C. L. Jiang, and K. E. Rehm, Rev. Mod. Phys. **86**, 317 (2014).
[14] Ş. Mişicu and H. Esbensen, Phys. Rev. Lett. **96**, 112701 (2006).
[15] Ş. Mişicu and H. Esbensen, Phys. Rev. C **75**, 034606 (2007).
[16] A. Diaz-Torres, D. J. Hinde, M. Dasgupta, G. J. Milburn, and J. A. Tostevin, Phys. Rev. C **78**, 064604 (2008).
[17] A. Diaz-Torres, Phys. Rev. C **82**, 054617 (2010).
[18] Takatoshi Ichikawa, Kouichi Hagino, and Akira Iwamoto, Phys. Rev. Lett. **103**, 202701 (2009).
[19] T. Ichikawa, Phys. Rev. C **92**, 064604 (2015).
[20] K. A. Brueckner, J. R. Buchler, and M. M. Kelly, Phys. Rev. **173**, 944 (1968).
[21] D. R. Hartree, Proc. Camb. Phil. Soc. **24**, 89 (1928).
[22] V. A. Fock, Z. Phys. **61**, 126 (1930).
[23] T. H. R. Skyrme, Phil. Mag. **1**, 1043 (1956).
[24] S. Hossain, A. S. B. Tariq, A. Nilima, M. S. Islam, R. Majumder, M. A. Sayed, M. M. Billah, M. M. B. Azad, M. A. Uddin, I. Reichstein, F. B. Malik, and A. K. Basak, Phys. Rev. C **91**, 064613 (2015).
[25] V. Y. Denisov and W. Nörenberg, Eur. Phys. J. A **15**, 375 (2002).
[26] Kouhei Washiyama and Denis Lacroix, Phys. Rev. C **78**, 024610 (2008).
[27] Cédric Simenel and Benoit Avez, Intl. J. Mod. Phys. E **17**, 31 (2008).
[28] C. Simenel, Eur. Phys. J. A **48**, 152 (2012).
[29] C. Simenel, M. Dasgupta, D. J. Hinde, and E. Williams, Phys. Rev. C **88**, 064604 (2013).
[30] D. Bourgin, C. Simenel, S. Courtin, and F. Haas, Phys. Rev. C **93**, 034604 (2016).
[31] K. Vo-Phuoc, C. Simenel, and E. C. Simpson, Phys. Rev. C **94**, 024612 (2016).
[32] Kouichi Hagino and Noboru Takigawa, Prog. Theo. Phys. **128**, 1001 (2012).
[33] A. S. Umar and V. E. Oberacker, Phys. Rev. C **74**, 021601 (2006).
[34] A. S. Umar, V. E. Oberacker, J. A. Maruhn, and P.-G. Reinhard, Phys. Rev. C **85**, 017602 (2012).
[35] K. Hagino, N. Rowley, and A. Kruppa, Comput. Phys. Commun. **123**, 143 (1999).
[36] C. R. Morton, A. C. Berriman, M. Dasgupta, D. J. Hinde, J. O. Newton, K. Hagino, and I. J. Thompson, Phys. Rev. C **60**, 044608 (1999).
[37] H. A. Aljuwair, R. J. Ledoux, M. Beckerman, S. B. Gazes,

J. Wiggins, E. R. Cosman, R. R. Betts, S. Saini, and O. Hansen, Phys. Rev. C **30**, 1223 (1984).
[38] G. Montagnoli, A. M. Stefanini, C. L. Jiang, H. Esbensen, L. Corradi, S. Courtin, E. Fioretto, A. Goasduff, F. Haas, A. F. Kifle, C. Michelagnoli, D. Montanari, T. Mijatoviç, K. E. Rehm, R. Silvestri, P. P. Singh, F. Scarlassara, S. Szilner, X. D. Tang, and C. A. Ur, Phys. Rev. C **85**, 024607 (2012).
[39] A. M. Stefanini, G. Montagnoli, R. Silvestri, L. Corradi, S. Courtin, E. Fioretto, B. Guiot, F. Haas, D. Lebhertz, P. Mason, F. Scarlassara, and S. Szilner, Phys. Lett. B **679**, 95 (2009).
[40] A. S. Umar and V. E. Oberacker, Phys. Rev. C **73**, 054607 (2006).
[41] Ka–Hae Kim, Takaharu Otsuka, and Paul Bonche, J. Phys. G **23**, 1267 (1997).
[42] A. S. Umar, M. R. Strayer, J. S. Wu, D. J. Dean, and M. C. Güçlü, Phys. Rev. C **44**, 2512 (1991).
[43] A. S. Umar, J. Wu, M. R. Strayer, and C. Bottcher, J. Comp. Phys. **93**, 426 (1991).
[44] V. Rotival and T. Duguet, Phys. Rev. C **79**, 054308 (2009).
[45] G.-H. Göritz and U. Mosel, Z. Phys. A **277**, 243 (1976).
[46] L. C. Chamon, B. V. Carlson, L. R. Gasques, D. Pereira, C. De Conti, M. A. G. Alvarez, M. S. Hussein, M. A. C. Ribeiro, E. S. Rossi, and C. P. Silva, Phys. Rev. C **66**, 014610 (2002).
[47] V. Y. Denisov and V. A. Nesterov, Phys. At. Nucl. **73**, 1142 (2010).
[48] V. A. Nesterov, Phys.Atom. Nucl. **76**, 577 (2013).
[49] N. Rowley and K. Hagino, Nucl. Phys. A **834**, 110c (2010).
[50] H. Esbensen and S. Landowne, Phys. Rev. C **35**, 2090 (1987).
[51] J. M. Yao and K. Hagino, Phys. Rev. C **94**, 011303 (2016).